LBL-19490

# Lawrence Berkeley Laboratory

UNIVERSITY OF CALIFORNIA

## Materials & Molecular Research Division

RECEIVED
LAWRENCE
BERKELEY LABORATORY
JUL 15 1985
LIBRARY AND
DOCUMENTS SECTION

Presented at the 167th Meeting of the
Electrochemical Society, Toronto, Canada,
May 12-17, 1985

# THE EFFECT OF FLOW OBSTACLES ON MASS TRANSFER TO PLANAR ELECTRODES

D.S. Fischl, R.H. Muller and C.W. Tobias

May 1985

TWO-WEEK LOAN COPY

This is a Library Circulating Copy
which may be borrowed for two weeks.

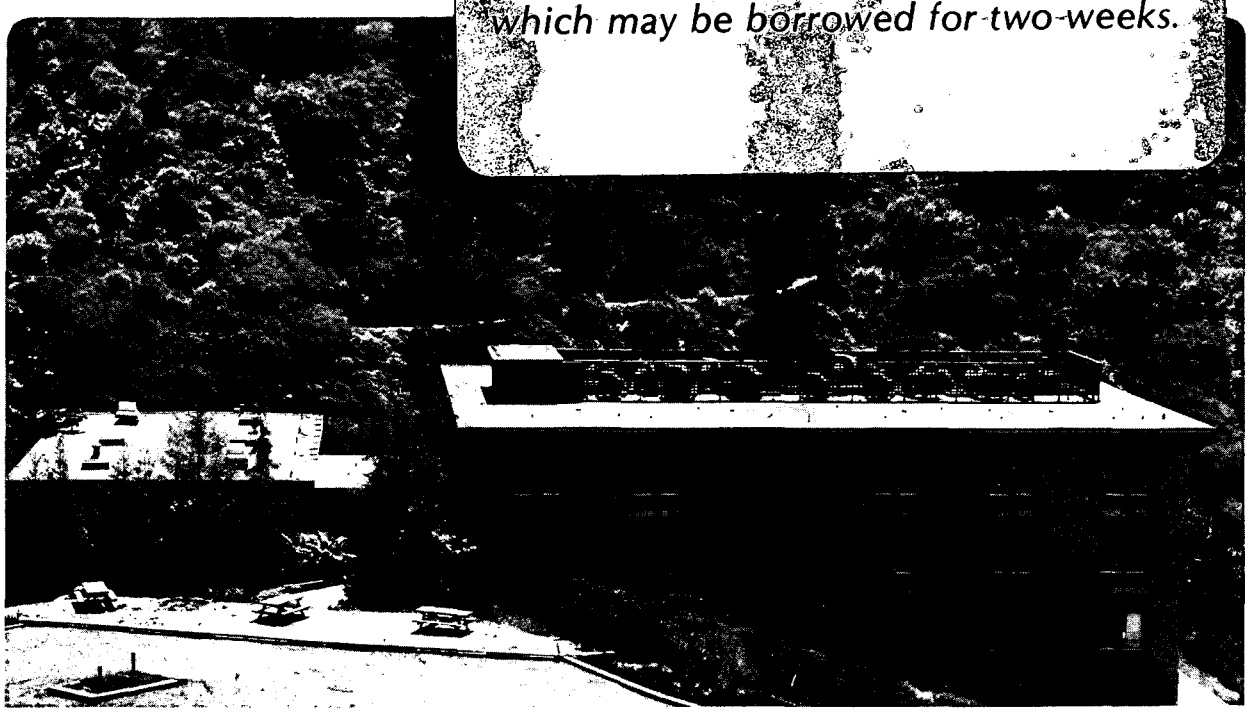

LBL-19490

Prepared for the U.S. Department of Energy under Contract DE-AC03-76SF00098

## DISCLAIMER

This document was prepared as an account of work sponsored by the United States Government. While this document is believed to contain correct information, neither the United States Government nor any agency thereof, nor the Regents of the University of California, nor any of their employees, makes any warranty, express or implied, or assumes any legal responsibility for the accuracy, completeness, or usefulness of any information, apparatus, product, or process disclosed, or represents that its use would not infringe privately owned rights. Reference herein to any specific commercial product, process, or service by its trade name, trademark, manufacturer, or otherwise, does not necessarily constitute or imply its endorsement, recommendation, or favoring by the United States Government or any agency thereof, or the Regents of the University of California. The views and opinions of authors expressed herein do not necessarily state or reflect those of the United States Government or any agency thereof or the Regents of the University of California.

# THE EFFECT OF FLOW OBSTACLES ON MASS TRANSFER TO PLANAR ELECTRODES

D.S. Fischl, R.H. Muller and C.W. Tobias

Materials and Molecular Research Division
Lawrence Berkeley Laboratory
and
Department of Chemical Engineering
University of California
Berkeley, CA 94720

## ABSTRACT

Mass transfer enhancement by rectangular rod shaped non-conducting obstacles attached to a planar electrode was investigated in a flow cell of 5x5 mm cross-section and 508 mm length, in the range of $80 < Re < 3200$. Effectiveness was evaluated for three different rod heights (0.25-1.6 mm) as a function of obstacle spacing by measuring both the pressure drop and the limiting current for the reduction of ferri-cyanide.

Recirculation flow patterns were visualized by a hydrogen bubble stream generated upstream from an obstacle. In the laminar flow regime, up to four-fold increase of mass transfer rate was obtained with a power demand for pumping that was as little as one-hundredth of that required for achieving the same transport rate in the unobstructed channel. Optimally spaced flow obstacles not only greatly enhance transport rates, they also prevent the progressive increase in mass transfer boundary layer thickness in the direction of flow.

# INTRODUCTION

When the rate of an electrode process is controlled by mass transfer to the electrode surface, such as when the concentration of the reacting species is low, flow obstacles can enhance the rate of convective diffusion at a fraction of the power demand for pumping the electrolyte faster, in the absence of obstructions (1-10). Improving transport rates (limiting currents) by increasing the rate of pumping between parallel planar electrodes is quite inefficient; in laminar flow the power requirement increases with the sixth power of the limiting current, while in turbulent flow the required power increases with approximately $I^{3.5}$.

Previous investigations have largely been focused on systems in which the obstacles were comparable in size to the interelectrode gap, or the inter-obstacle spacing was small. Interferometric observations in this laboratory have clearly demonstrated that obstacles with diameters much smaller than the interelectrode gap may cause considerable thinning of the mass transfer boundary layer over extended distances downstream [11,12]. Close spacing of obstacles such as in the Swiss Roll Cell [7,8] may therefore reduce the effectiveness of the secondary convection following an obstacle. Close spacing also results in excessive shielding of the electrode.

The question arises then: how close should obstacles be placed for maximum enhancement of transport rates, along with minimal coverage of the electrode surface, and what is the resulting pressure

drop (or required pumping power)? In the following, experimental results are reported for rectangular prism-shaped rods with large spacing, attached to the cathode, in a channel-type electrolytic cell, in which the gap/obstacle height ratio ranged from 3 to 20.

## APPARATUS AND EXPERIMENTAL PROCEDURE

A diagram of the flow system is presented in Fig. 1. Electrolyte flow through the channel was driven from the holding tank by gravity or by positive nitrogen pressure. The piping was constructed of black polypropylene tubing. A needle valve was used to adjust the flow rate, which was measured by a rotameter. The unobstructed flow channel had a 5x5 mm cross-section with parallel nickel electrodes (approximately 50.8 cm in length) forming the upper and lower walls. The side walls were constructed of acrylic resin.

To evaluate the cumulative effect of regularly spaced obstacles on the average mass transfer coefficient, the limiting current technique [13] was employed for the cathodic reduction of ferri-cyanide on the upper nickel electrode. The electrolyte was 0.01 M $K_3Fe(CN)_6$ and 0.05 M $K_4Fe(CN)_6$ in a 0.30 M NaOH supporting electrolyte solution. A PAR 371 potentiostat was used for control of the applied potential and a Data Precision Model 1455 ammeter monitored the current passing through a cell. The diffusivity of the reacting $Fe(CN)_6^{3-}$ ion was calculated using the correlation by Gordon [14]. The pressure drop was measured between two pressure taps machined into a side wall of the cell

halfway between the electrodes at the leading and trailing edges. A diaphragm type pressure transducer (Validyne DP103) was used to monitor the pressure differences between these two sampling points.

The flow obstacles were cut out of acrylic resin and attached with an adhesive directly to the cathode extending fully across the width of the channel. Figure 2 shows the geometric relationship between the electrode gap and obstacle size. The majority of the experiments were performed with the 0.76 and 1.6 cm size obstacles in the Reynolds numbers range of 80 to 3,200. The total number of equally spaced obstacles attached to the 50.8 cm long electrode ranged from 1 to 49 with none located at the leading or trailing edge of the electrode. Data on channel geometry are summarized in Table I; results are presented using the number of obstacles as the parameter. Further details on the experimental procedures have been reported elsewhere [15].

## RESULTS

The results and conclusions presented in this paper have been largely derived from measurements involving 1.6 and 0.76 mm obstacles, for which the majority of pressure drop and limiting current data were obtained. Because of the much more limited scope of experiments with the smallest obstacles (0.25 mm) only tentative conclusions can be offered related to these.

The total current at Re = 691 as it depends on the number of

1.6x1.6x5 mm obstacles and applied voltage is shown in Figs. 3. Figure 4 shows the effect of the number of obstacles and flow rate on the limiting current, $I_L$. A dramatic increase due to the presence of obstacles is clearly evident. It is also quite apparent that although increasing the frequency of obstacles enhances the average mass transfer rate to the electrode surface, once the rods are placed relatively close together, further crowding brings about no beneficial effect. While in the case of 1.6 mm rods, 15 of these causes a greater increase in $I_L$ than 31, using 0.76 m rods the optimal number is much higher (31 vs. 15) indicating that the optimal spacing is related to the cross-section of the rods employed. Although the maximum mass transfer enhancement observed is approximately the same for these two sizes, the smaller obstacles present less resistance to fluid flow (lower pressure drop) and provide therefore a greater overall benefit. In the case of the smallest (0.25 mm) rods, the pressure drop is further reduced, however, along with a more than proportionate decrease in transport enhancement.

The dependence of $I_L$ on the Reynolds number and on obstacle spacing (Fig. 4) clearly shows that the relative enhancement increases with Re in the laminar regime. A dimensionless plot of the Sherwood number as it depends on Reynolds and Schmidt numbers, and on the ratio of hydraulic diameter of the duct ($D_e$) to the electrode length (L) is shown in Fig. 5. The analytic correlation in the laminar flow regime in an unobstructed channel is also shown for comparison [16].

For a given rod spacing, the mass transfer rate enhancement increases with Re until the region of incipient turbulence is reached. This condition is reached at lower Re as the obstacle size is increased. With fifteen 1.6 mm obstacles incipient turbulence is evident already at Re = 400. At higher flow rates bulk turbulence develops and the relative contribution of obstacles to mass transfer enhancement diminishes. Results of pressure drop measurements, shown in Fig. 6, allow the evaluation of the power required for pumping as it depends on rod size and spacing. Although at low flow rates the addition of obstacles do not significantly increase the pressure drop, at higher flow rates exponential dependence on velocity is observed and the pressure drop sharply increases upon the addition of obstacles. This effect, along with a lack of proportionate increase in mass transfer enhancement upon closer spacing of obstacles, leads to the conclusion that an optimum spacing exists, which depends on rod size. Using 1.6 mm rods, fifteen of these spaced at 23.4 times diameter, produced the most beneficial enhancement. For the 0.76 mm rods the optimal spacing was 21 times rod diameter, corresponding to 31 rods spaced evenly over 50 cm. At Re = 100 the mass transfer rate is approximately doubled without appreciably affecting the pressure drop. A four-fold increase of $I_L$ occurs at Re = 1000 along with only a four-fold increase in pressure drop relative to the open channel.

The dependence of the Fanning friction factor on the Reynolds number in the presence of flow obstacles is shown in Fig. 7. The line for laminar flow without obstacles is shown for comparison [18].

## HYDRODYNAMICS

It is evident that the addition of obstacles enhances mass transfer by changing the flow pattern near the electrode surface. Such patterns for the 0.16x0.16x0.50 cm obstacles were observed and photographed using a stream of small hydrogen bubbles generated upstream on a wire or mesh electrode. In Fig. 8, the gradual extension of the recirculation zone with increase in Reynolds number is shown downstream from an obstacle. Recirculation zones have been observed and described earlier in relation to an investigation concerning the nature of flow downstream from a step [19,20] or obstacle [9,10] in a channel.

The length of the recirculation zone increases with increasing flow rate. The elongation continues to increase with flow velocity until bulk turbulence is produced. Smaller obstacles produce a disturbance that extends over a shorter length downstream, with bulk turbulence occurring at a higher flow rate. Further visualization experiments were performed to observe the effect of obstacle spacing. With 31 (0.076x0.076x0.5cm) obstacles attached to the electrode the recirculation zone almost reached the next downstream obstacle. With 49 obstacles, the recirculation zone extended over the entire inter-obstacle distance and interacted with the next downstream obstacle. Before incipient bulk turbulence was observed in all the arrangements, the flow in the bulk was essentially laminar, while close to the wall behind the obstacle extensive mixing was produced

by the swirling recirculation zone. These results are consistent with previous investigations where the maximum elongation of the recirculation zone in the laminar regime was believed to be approximately 15 times the obstacle height [10].

Subsequent to the experimental study described above, the Navier Stokes equations describing flow for the two dimensional case of flow past an obstacle in a channel of infinite width had been solved numerically. The solution was obtained by using the finite element code POLYFLOW [21] developed at the Universite Catholique in Louvain-la-Neuve, Belgium. The dimensions were chosen to be geometrically equivalent to the obstacles used in the experimental study. The solution is only valid for the laminar flow regime and cannot be used to predict or describe the turbulent transition. The numerically generated streamlines are presented in Fig. 9 for various Reynolds numbers. These streamlines agree qualitatively with those observed in the flow visualization experiments.

## DISCUSSION

An analysis of benefits derived from the use of small flow obstacles has to be based on the pumping power requirement rather than on the pressure drop alone. The specific pumping power requirement per unit cathode area is a product of the volumetric flow rate times the pressure drop divided by the electrode area. The specific power as a function of achieved mass transfer rate (limiting

current density) is shown in Fig. 10 for the unobstructed and multiple obstacle cases. When higher currents (mass transfer rates) must be achieved in the unobstructed channel, the required power for pumping increases proportionally to $I_L$ in the laminar regime, and with $I_L^{3.5}$ in turbulent flow. In order to obtain total currents over approximately 18 mA (shown in Fig. 3) corresponding to mass transfer coefficients larger than $0.8 \times 10^{-1}$ cm $cec^{-1}$ a large increase of the required pumping power in the unobstructed channel is required because the bulk flow must be turbulent.

In Fig. 10, the enhancement effect provided by an optimal number of 0.76 mm obstacles is compared to the highest enhancement effect found for 1.6 mm obstacles. In the presence of 31 evenly spaced 0.76 mm obstacles, the pumping power required to achieve a K = $7 \times 10^{-4}$ cm/sec ($I_L$ = 0.7 mA/cm$^2$) is only approximately one hundredth of that required for achieving the same mass transfer rate in the absence of obstacles. A limiting current of 3 mA/cm$^2$ could be achieved in the open channel only in turbulent bulk flow; however, when the channel is obstructed by 31 0.76 obstacles the same limiting current can be achieved (in laminar bulk flow), at a power requirement that is eleven times lower. It is interesting to note that in this regime the power demand for pumping in the channel obstructed with either the 0.76 or 1.6 mm obstacles increases with $I_L^{4.3}$. At lower flow rates, (below K = $10^{-3}$ cm/sec), the dependence of power demand on limiting current, with or without obstacles, is similar or approximately proportional to $I_L^6$.

## CONCLUSIONS

Attached small obstacles have been shown to increase the rate of mass transfer to the walls of a flow channel. Reducing the spacing between the obstacles produces increased mass transfer enhancement; however, when the spacing is too close, effectiveness is decreased. For rectangular rod-shaped obstacles, the optimum spacing is approximately 15-25 times the obstacle height; this corresponds to the maximum elongation of the downstream recirculation zone. Compared to the unobstructed channel, the obstacles provide a more uniform current distribution and a considerable reduction in the pumping power required to achieve a given average rate of mass transfer. The advantage of flow obstacles diminishes in bulk turbulent flow because of the loss of benefit derived from recirculation type mixing close to the wall when the bulk fluid itself is turbulent.

## ACKNOWLEDGMENT

This work was supported by the Director, Office of Energy Research, Office of Basic Energy Sciences, Materials Sciences Division of the U.S. Department of Energy under Contract Number DE-AC03-76SF00098.

Table I. Channel Geometry

| Obstacle Size (mm) | Number of Obstacles | Ratio of Obstacle Spacing to Obstacle Height | Ratio of Obstacle Spacing to Hydraulic Diameter | Active Electrode Area ($cm^2$) |
|---|---|---|---|---|
| - | 0 | - | - | 24.2 |
| 0.25x0.25 x5 | 15 | 125 | 6.9 | 23.6 |
| 0.76x0.76 x5 | 3 | 166.67 | 27.6 | 24.1 |
| | 15 | 41.67 | 6.9 | 23.6 |
| | 31 | 20.73 | 3.4 | 23.0 |
| | 49 | 13.39 | 2.2 | 22.3 |
| 1.6x1.6 x5 | 1 | 158.75 | 55.2 | 24.1 |
| | 3 | 79.37 | 27.6 | 24.0 |
| | 7 | 39.69 | 13.8 | 23.7 |
| | 15 | 23.44 | 6.9 | 23.1 |
| | 31 | 9.87 | 3.4 | 22.0 |

# FIGURE CAPTIONS

1. Schematic of flow system.
2. Geometric relations between obstacles and electrode gap.
3. Limiting current curves for the 0.16 cm obstacles Re = 691. 25 mV increments applied every 15 seconds. Curves smoothed by illustrator.
4. Limiting current as a function of flow rate. Note that increasing the number of obstacles from 15 to 31 does not increase the limiting current.
5. Dimensionless plot of mass transfer rates. Note that the analytic solution [16] for the unobstructed duct is only valid for the laminar regime.
6. Pressure drop as a function of flow rate and number of obstacles. Linear relationship for laminar flow in the unobstructed duct indicated by solid line [18].
7. Dependence of the measured friction factor on Reynolds number. Solid line depicts the analytic solution for the laminar flow regime in a square.
8. Flow patterns downstream from 1.6x1.6 mm obstacles. Hydrogen bubbles tracing the flow paths were generated upstream from the obstacle.
9. Numerically generated streamlines around an obstacle for two different Raynolds numbers.
10. Specific power requirement for fifteen 1.6x1.6 mm of thirty-one 0.76x0.76 mm obstacles as a function of limiting current density of mass transfer coefficient. Solid lines describe behavior in the absence of obstacles.

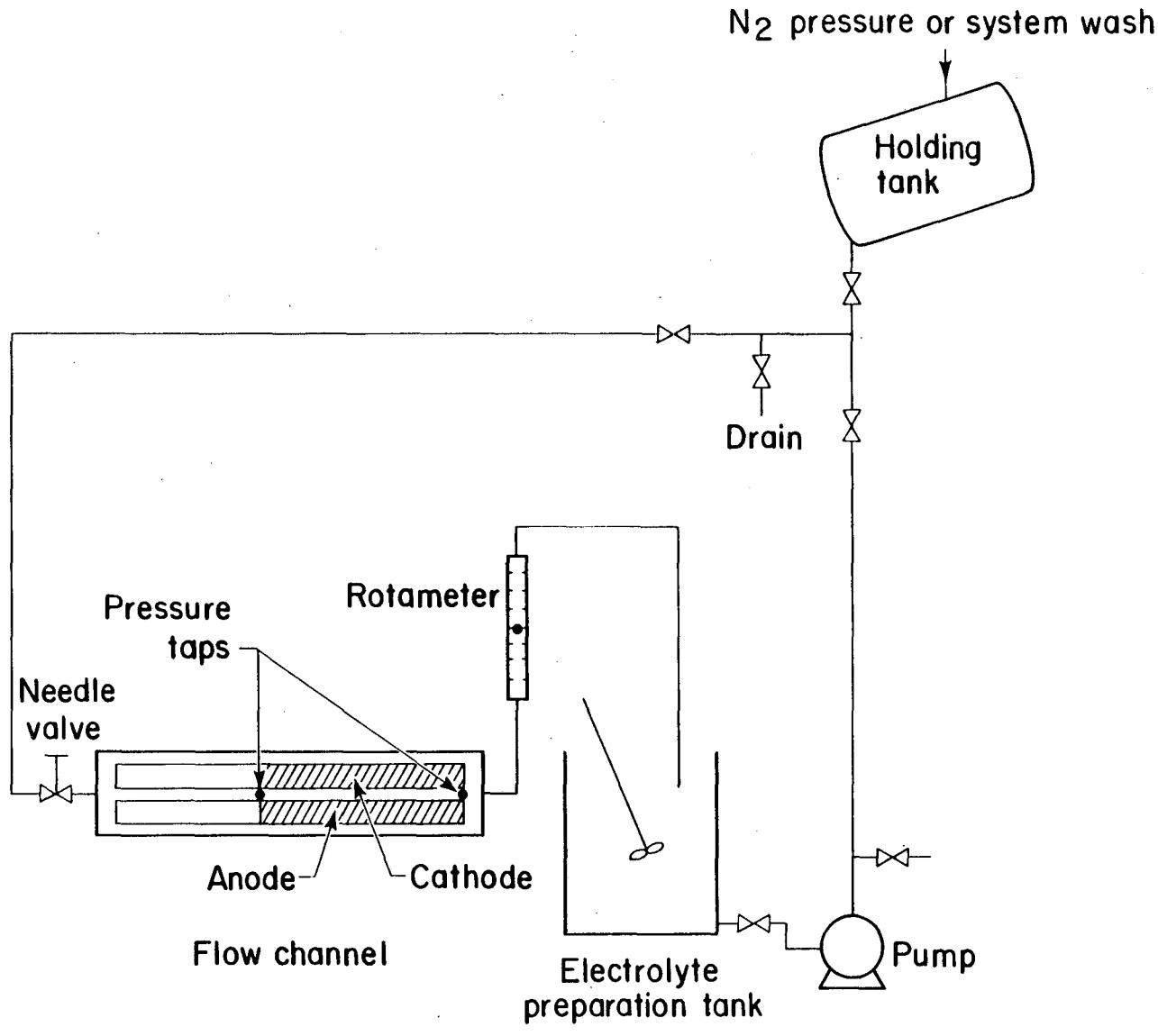


XBL 837-2817

Fig. 1

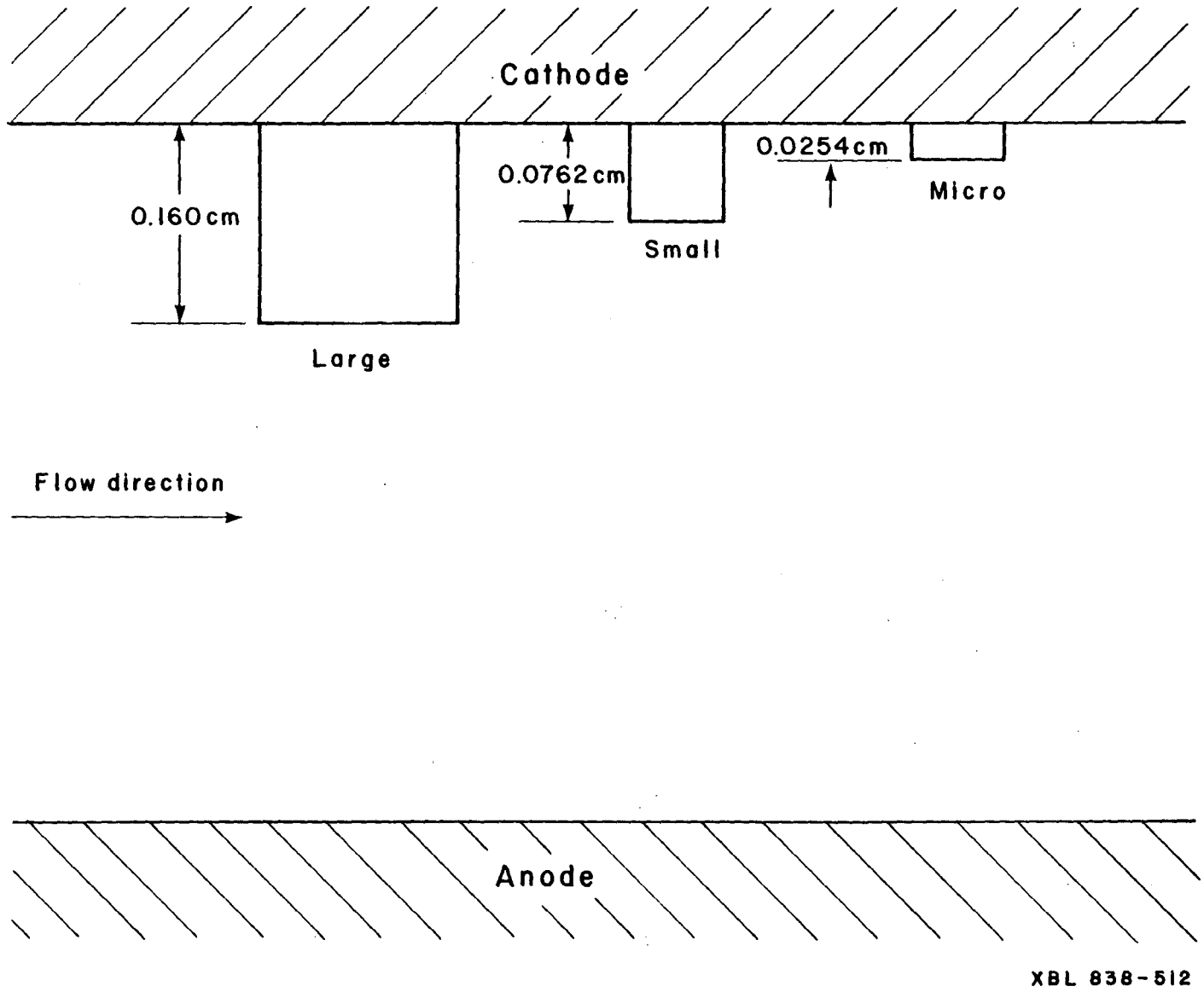
Cathode
0.160cm
Large
0.0762cm
Small
0.0254cm
Micro
Flow direction
Anode
XBL 838-512

Fig. 2

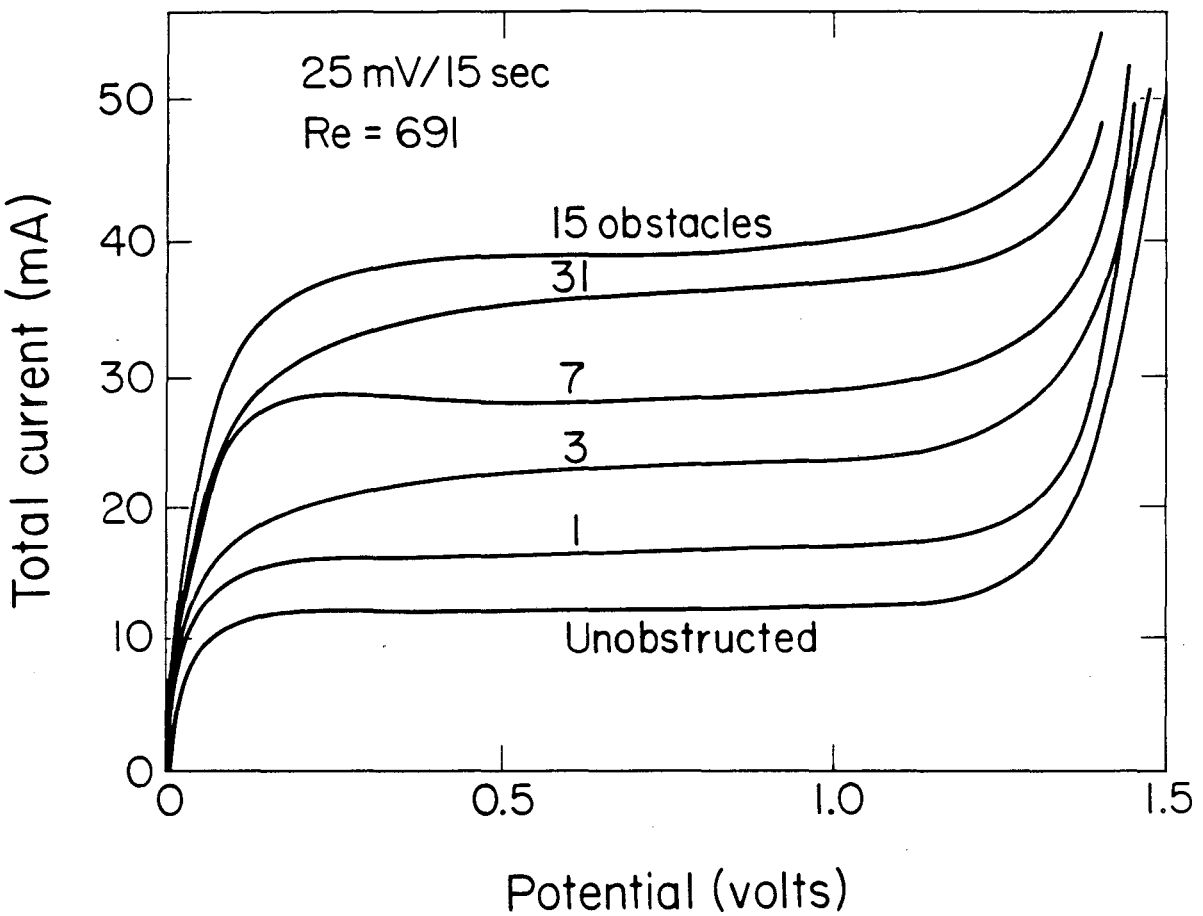


XBL 835-2635

Fig. 3

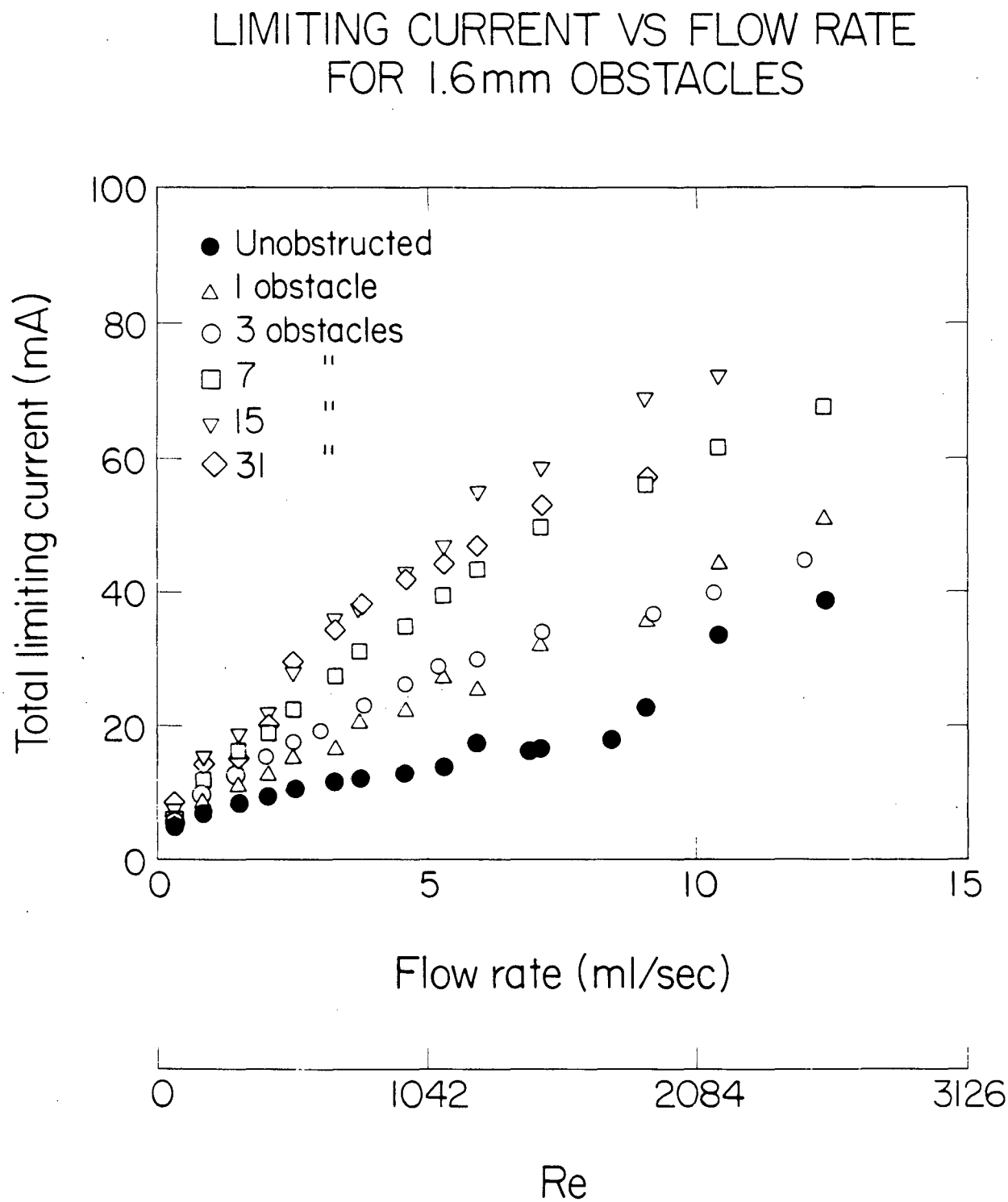


XBL 838-10936

Fig. 4

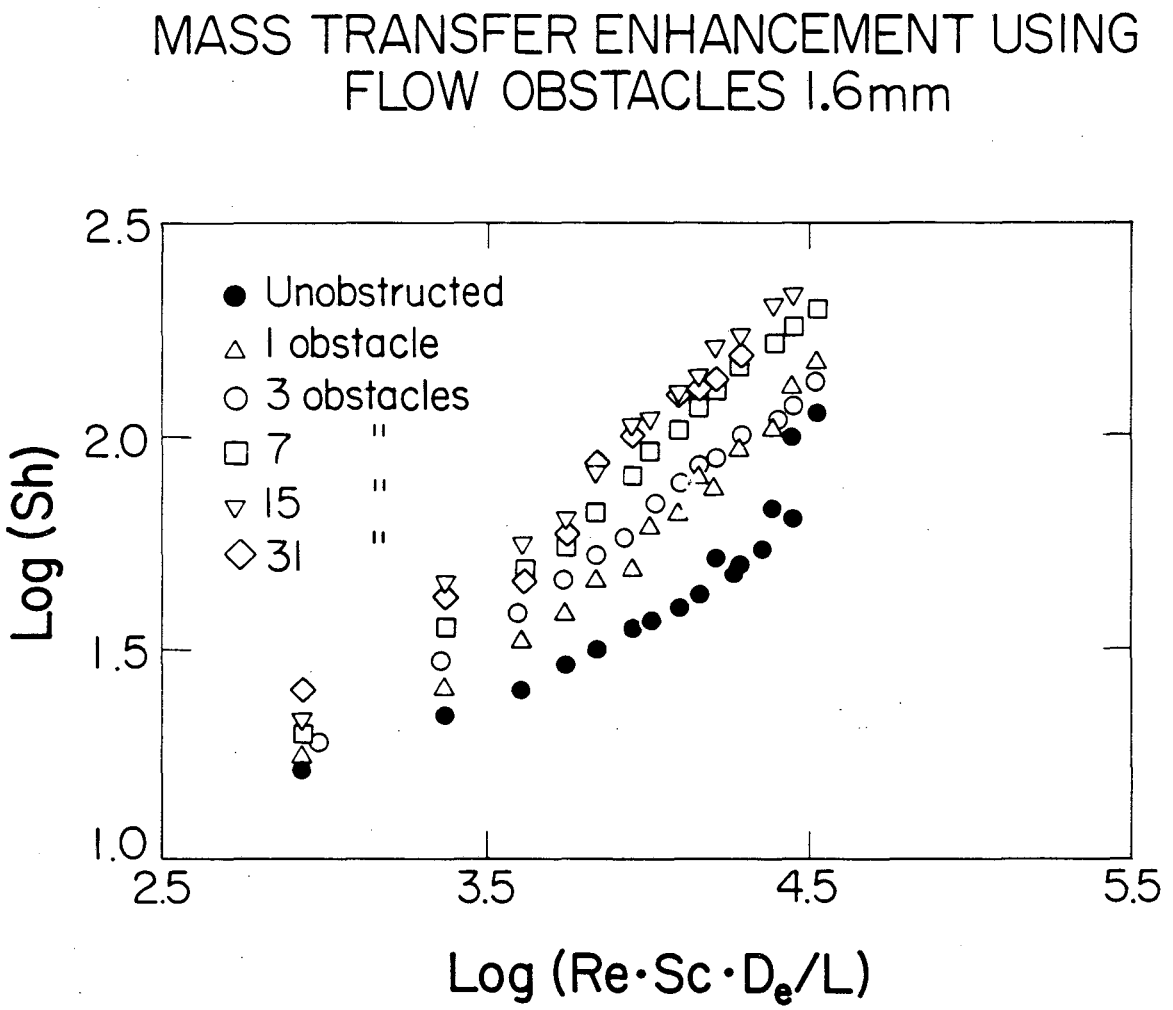


XBL 837-2776

Fig. 5

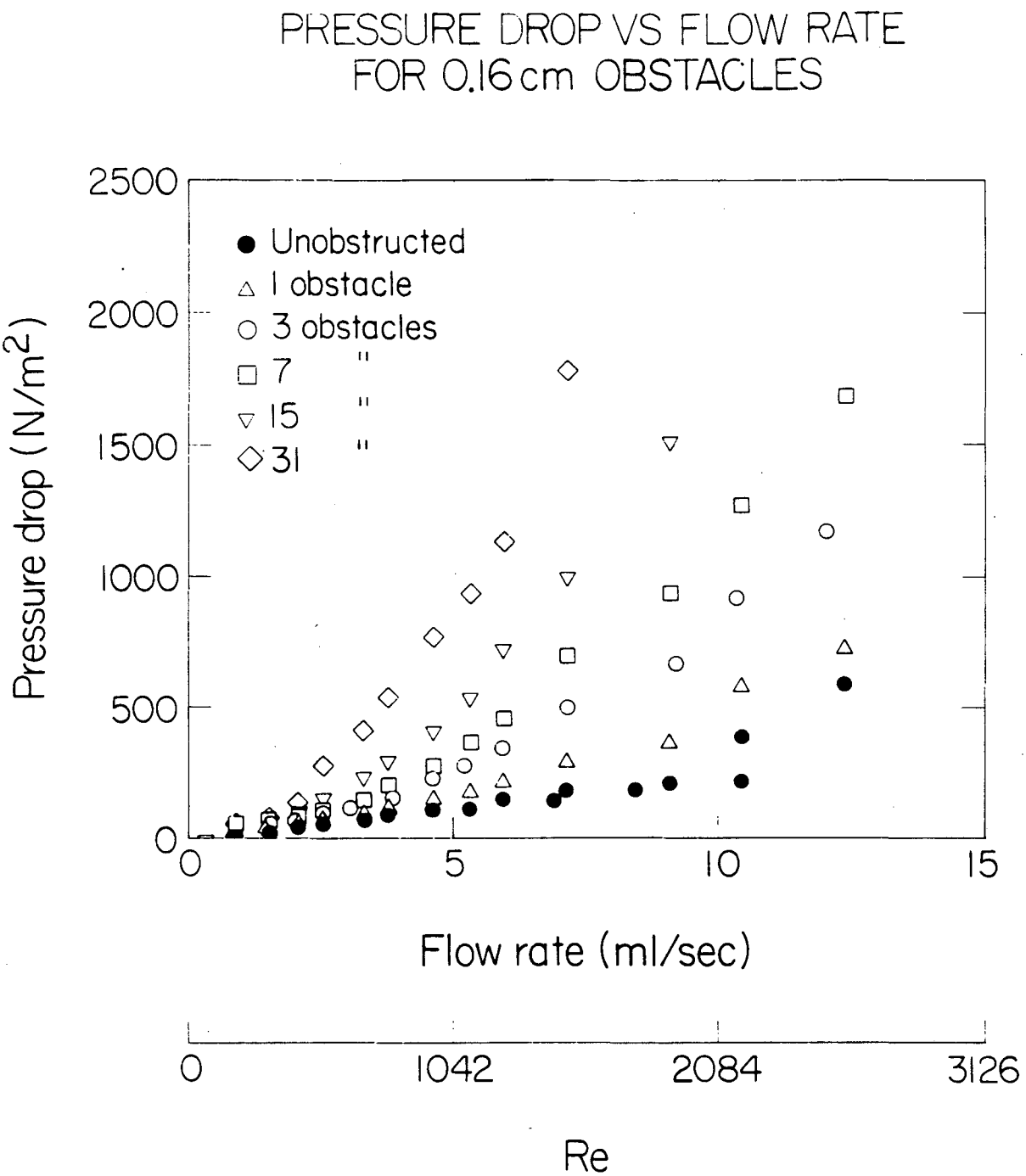


XBL 838-10937

Fig. 6

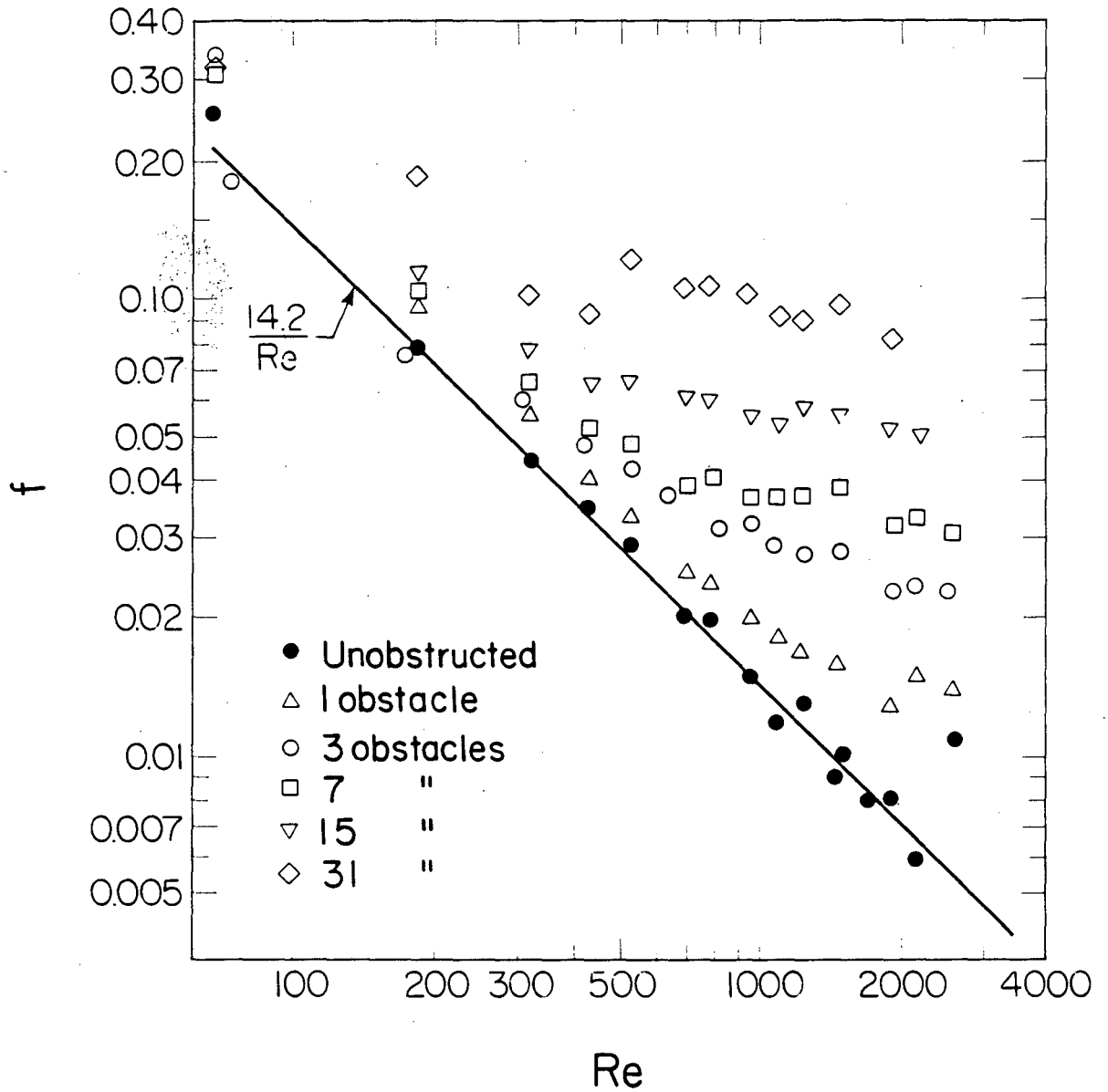


XBL 837-2821

Fig. 7

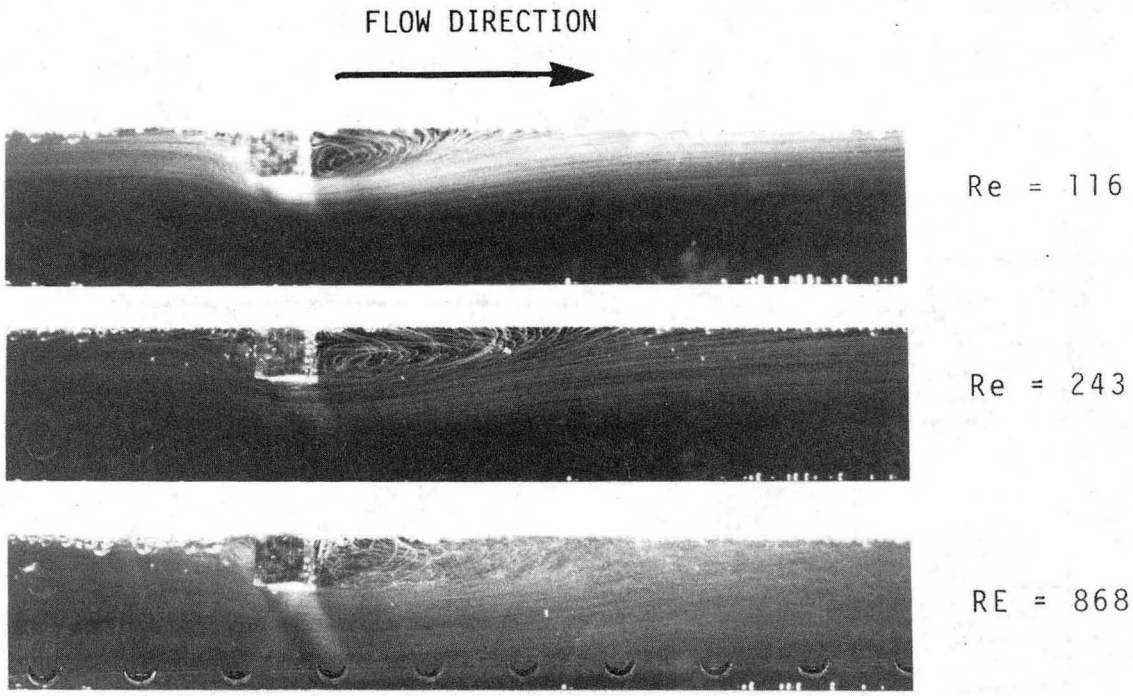


Fig. 8

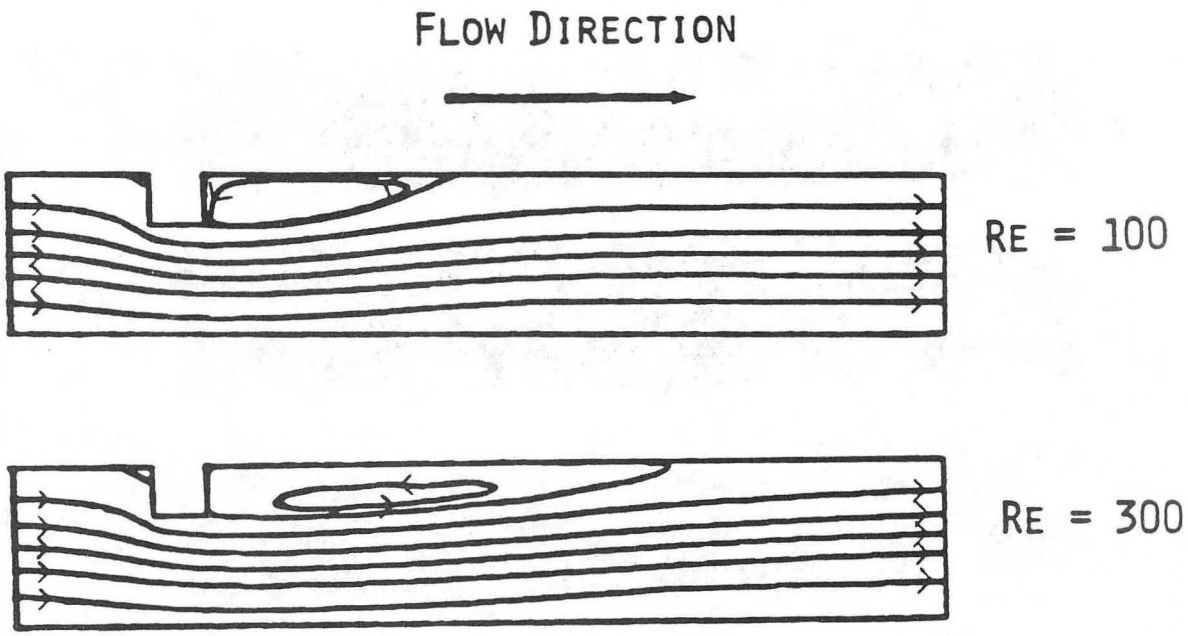


XBL 855-2427

Fig. 9

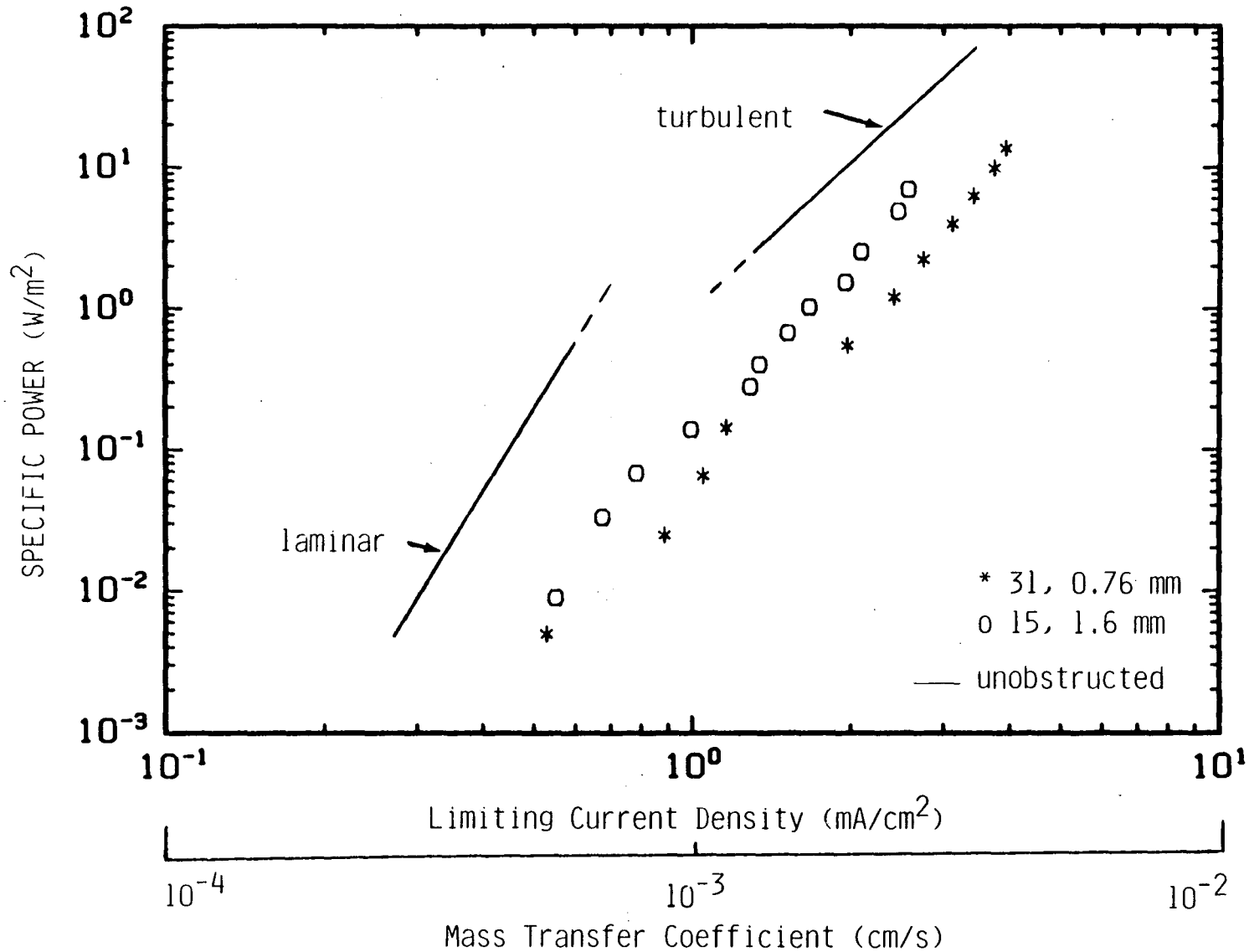


XBL 855-2428

Fig. 10

## REFERENCES


1. A. Solan, Y. Winograd and U. Katz, Desalination 9, 89 (1971).
2. A.A. Sonin and M.S. Isaacson, Ind. Eng. Chem. Proc. Des. Dev., 13, 241 (1974)
3. F.B. Leitz and L. Marincic, J. Appl. Electrochem., 7, 473 (1977).
4. J.J.S. Shen and R.F. Probstein, Ind. Eng. Chem. Proc. Des. Dev. 18, 597 (1979).
5. A. Storck and F. Coeuret, Ind. Eng. Chem. Proc. Des. Dev. 17, 99 (1978).
6. A. Storck and D. Hutin, Electrochim. Acta 26, 117, 127 (1981).
7. P.M. Robertson and N. Ibl, J. Appl. Electrochem. 7, 323 (1977).
8. F. Schwager, P.M. Robertson and N. Ibl, Electrochim. Acta 25 1655 (1980).
9. I.S. Kang and H.N. Chang, Int. J. Heat Mass Trans., 25, 1167 (1982).
10. W.W. Focke, Electrochim. Acta 28, 1137 (1983).
11. F.R. McLarnon, Ph.D. Thesis, Dept. Chem. Engr., University of California, Berkeley, CA, 1975. (LBL-3500)

12. K.J. Hanson, M.S. Thesis, Dept. of Chem. Engr., University of California, Berkeley, CA, 1979. (LBL-9038)

13. J.R. Selman and C.W. Tobias, J. Electroanal. Chem., 65, 67 (1975).

14. S.L. Gordon, J.S. Newman and C.W. Tobias, Ber. Bunsenges. Phys. Chem., 70, 414 (1966).

15. D.S. Fischl, M.S. Thesis, Dept. of Chem. Engr., University of California, Berkeley, August 1983. (LBL-16422)

16. I. Rousar, J. Hostomsky and V. Lezner, J. Electrochem. Soc., 118 881 (1971).

17. H.F.P. Purday, Streamline Flow, Constable, London (1949) p. 14.

18. F.M. White, Viscous Fluid Flow, McGraw-Hill, NY, (1974) p. 123.

19. R.E. Chilcott, Int. J. Heat Mass Transfer, 10, 783-797, (1967).

20. R.J. Goldstein, V.L. Eriksen, R.M. Olson and E.R.G. Eckert, J. of Basic Engineering, 92, 732 (1970).

21. M.J. Croche Polyflow Users Manual and Theoretical Background, Unite de Mecanique Appliquee, Batiment Stevin, Place du Levan, 2, 1348 Louvain-la-Neuve, Belgium (Sept. 1982).

## Key Words for Subject Index

Fischl, et al., "The Effect of Flow Obstacles on Mass Transfer to Planar Electrodes"


| | |
|---|---|
| p. 1 | flow obstacles |
| p. 1,4 | mass transfer enhancement |
| p. 2,6 | pumping power |
| p. 2 | boundary layer thinning |
| p. 3 | limiting current |
| p. 3,4 | pressure drop |
| p. 4 | Fanning friction factor |
| p.4 | flow pattern |
| p. 4,5 | recirculation zone |
| p. 5 | flow visualization |

This report was done with support from the Department of Energy. Any conclusions or opinions expressed in this report represent solely those of the author(s) and not necessarily those of The Regents of the University of California, the Lawrence Berkeley Laboratory or the Department of Energy.

Reference to a company or product name does not imply approval or recommendation of the product by the University of California or the U.S. Department of Energy to the exclusion of others that may be suitable.

*LAWRENCE BERKELEY LABORATORY*
*TECHNICAL INFORMATION DEPARTMENT*
*UNIVERSITY OF CALIFORNIA*
*BERKELEY, CALIFORNIA 94720*